

# High-Precision 2.4 GHz DSSS RF Ranging

Bradley D. Farnsworth, David W.A. Taylor  
Advanced Projects and Applications Division  
ENSCO, Inc.

## BIOGRAPHY

Bradley D. Farnsworth (farnsworth.bradley@ensco.com) is a senior engineer at ENSCO. He was the sensors technical lead for the national semifinalist Team Case for the 2007 DARPA Urban Challenge and won a Best Student Paper award at the 2008 IEEE Sensors Conference. Mr. Farnsworth holds the B.S. *summa cum laude* and M.S. degrees in Electrical Engineering from Case Western Reserve University.

Dr. David W.A. Taylor (taylor.david@ensco.com) is ENSCO's Director of Technology Development, where he leads the company's R&D programs developing sensors and systems for national security applications. Dr. Taylor holds three U.S. patents and is an expert in GPS-denied navigation technologies. Dr. Taylor holds the B.S. in Physics from Rhodes College and the Ph.D. in Geophysics from Virginia Tech.

## ABSTRACT

Precision ranging radios are a critical aid to integrated locating, tracking, navigation, and guidance systems, especially when GPS service is degraded or unavailable [5]. In this work, a high-precision, software-defined, round-trip time-of-flight, direct sequence spread spectrum (DSSS) ranging radio operating in the 2.4 GHz ISM band is presented. This system builds upon our previous brassboard implementation at 915 MHz [1, 2], and continues ENSCO's decade-long research in this area [6, 7] with system enhancements bringing the performance closer to the Cramer-Rao Lower Bound for round-trip DSSS time-of-flight ranging.

The system is capable of performing 217 independent range measurements per second with measurement standard deviation as low as 2.5 cm in a benign line-of-sight RF environment. The system achieves high distance linearity and low intercept offset using a single-point calibration method. The ranging performance has been characterized at distances in excess of 1 kilometer and in indoor line-of-sight situations.

## INTRODUCTION

This distance-measuring system consists of a pair of radios designated Originator and Transponder. These radios have an identical hardware, software, and firmware implementation with roles designated through software configuration. The Originator begins each transaction by transmitting a pre-defined message structure including a preamble, a synchronization word, and a data payload [1]. The Transponder receives this message and then transmits a locally-generated version of the message with its own data payload upon complete reception of the first message. The Originator then receives this second message to complete the round-trip operation.

Coarse timing is achieved by counting clock cycles between received and transmitted (or between transmitted and received) synchronization words in both radios. The difference in dwell times in both radios provides a coarse estimate of round-trip time-of-flight.

Sub-clock cycle timing is achieved through estimation and tracking of the time offset between the centroid of each correlator output pulse and the sampled peak. This baseband phase estimate at the instant each synchronization word is received constitutes the fine timing correction factor. By estimating the baseband phase for each symbol received during the tracking period and tracking this phase estimate over time, offsets of the free-running baseband clocks are directly observed and corrected.

The combination of the coarse counts between synchronization words in both radios with the corresponding baseband phase correction factors and a calibrated offset provide a precise round-trip time-of-flight estimate.

## SYSTEM IMPLEMENTATION

Each radio is implemented as a two-board stack-up with a motherboard that implements the analog and digital baseband and a daughterboard consisting of a custom half-duplex direct-conversion 2.4 GHz BPSK transceiver

implementation with +20 dBm RF transmit power. The radio development platform is shown in Figure 1.



**Figure 1. Distance Measuring Radio Development Platform**

The digital baseband processor is implemented using MATLAB Simulink with the Xilinx System Generator and runs in a Xilinx VIRTEX-5 FPGA. A TI MSP430 microcontroller handles system initialization and configuration. A high-speed USB2 interface provides an interface to complete range measurements as well as high-speed intermediate baseband data for development purposes including raw A/D samples and de-spreading correlator output data at the baseband sample rate of 44 million samples per second.

Spread-spectrum signaling is used in order to achieve a system processing gain. A Barker-13 spreading code is selected for its autocorrelation properties [1]. The chipping rate is 11 million chips per second and each Barker code is zero-padded to a total length of 17 chips, so the baseband digital data rate is approximately 650 thousand bits per second. The baseband signal is filtered to occupy a spectral bandwidth of approximately 22 MHz. The baseband signal is 4x oversampled at 44 MHz to enable improved time resolution.

Software to interface with the distance measuring radios over a high-speed USB2 connection has been developed in Python, LabVIEW, and the open-source OSSIE software-defined radio platform [8].

## TEST RESULTS

The distance measuring radio system has been characterized in a variety of environments. An outdoor test in an open field was performed to evaluate the radio's measurement standard deviation performance and linearity. These data sets are presented in Figure 2 and Figure 3, respectively. These measurements were performed using a patch antenna on the Originator at about 3 meters off the ground and an omni-directional

antenna on the Transponder directly attached to the radio's SMA connector and held at about 1.5 meters off the ground by the experimenter.

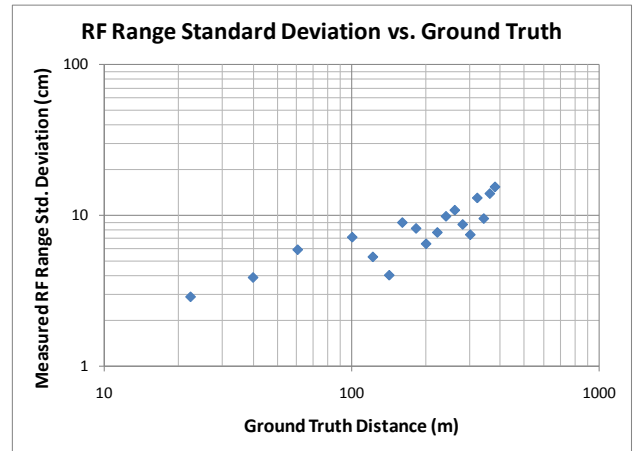


**Figure 2. Static Standard Deviation Measurements in Open Field**

From the data in Figure 2, it can be seen that the measurement standard deviation was always better than 20 cm within the testing distance of 400 meters, and as low as 3 cm. This level of performance is repeatable in environments with low multipath channel effects.

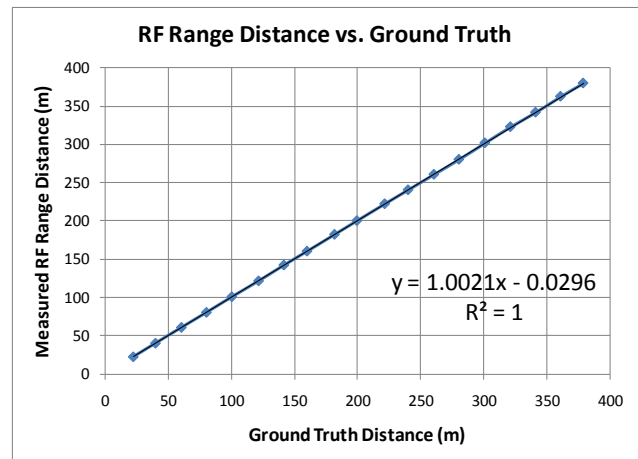


**Figure 3. Static Distance Measurements in Open Field**

The data in Figure 3 show that the distance measurement is very linear with a low intercept offset. The single-point calibration for this data set was performed at 20 meters offset at the beginning of the test to determine a single value to subtract off all time-of-flight measurements to account for system delays.

A zoomed-in view of RF range data collected at 217 Hz is presented in Figure 4. This data set of 13,064 points over one second was collected in the same manner as in Figures 2 and 3 with a patch antenna on the Originator and an omni-directional antenna directly attached to the Transponder with a 25.7 meter offset between the

antennas. The data shows a standard deviation of 3.6 cm and is representative of outdoor range data in a low multipath environment.

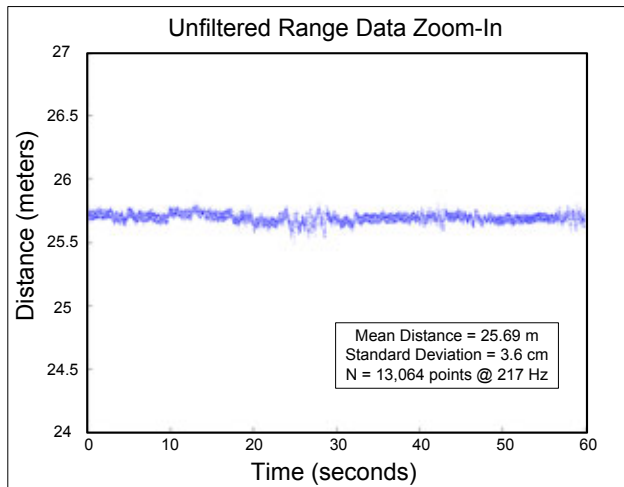


**Figure 4. Unfiltered Static Data in Open Field**

To demonstrate the system under dynamic conditions, the Transponder was mounted inside a convertible car and the Originator was placed at the end of a long, straight road. Data was collected using omni-directional antennas on both radios with the Originator’s antenna mounted at about 3 meters off the ground and the Transponder’s antenna mounted directly to the radio’s SMA connector, with the radio held above the windshield. The road and test setup is shown in Figure 5, although the photo shows a patch antenna on the mast that was not used in this data set. A chain link fence, dense foliage, and telephone poles lined the length of the road.

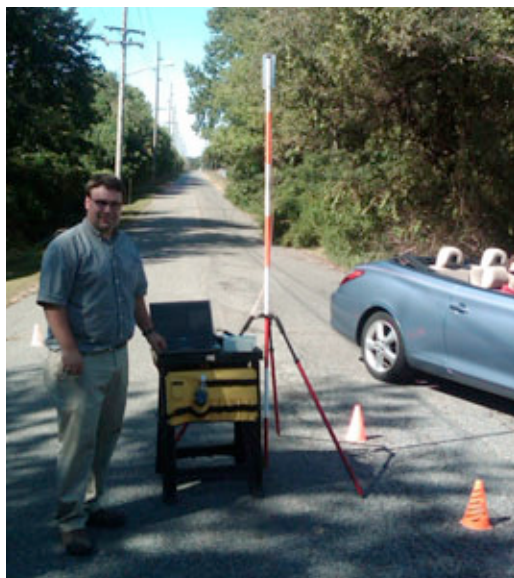


**Figure 5. Outdoor Driving Test Site**

In this test, the car started out near the fixed Originator position and then accelerated down the road until it went

over the line-of-sight horizon. At that point, the car turned around and accelerated back towards the Originator. During this test, the car traveled at over 50 MPH. There was no ground truth recorded for this data set, but the raw, unfiltered measurement data are presented in Figure 6.

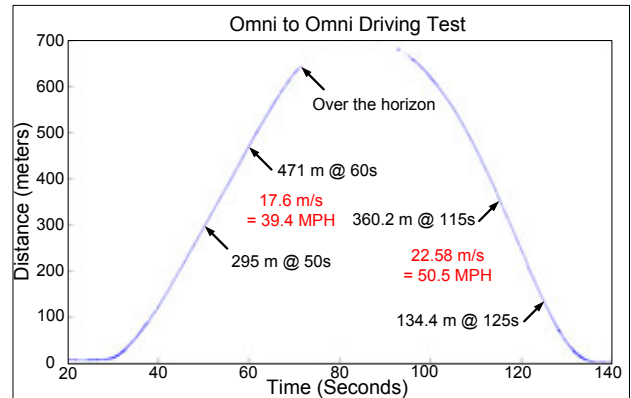


**Figure 6. Outdoor Driving Measurement Data**

A similar test was performed on a freshwater lake using a ski boat as shown in Figure 7. In this test, the Originator radio was placed on the dock at the shore with a patch antenna at about 3 meters above the water surface. The Transponder omni-directional antenna was mounted on a pole in the center of the ski boat at about 3 meters above the water surface. In addition, a NovAtel L1 GPS receiver was used to log GPS ground truth for the ski boat’s location at 20 Hz with timestamps synchronized with the RF range data.

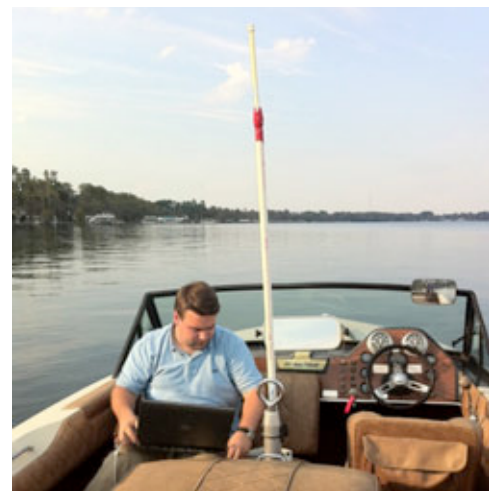


**Figure 7. Ski Boat Test**

In this test, the boat began near the dock and then accelerated away across the lake. Due to the high angle of attack of the ski boat at the high speeds used in this test of about 30 MPH, the Transponder’s omni-directional antenna was not normal to the water. At larger distances, this caused the measurements to drop out more often

than was observed when the boat was stationary or moving slowly. However, at the apex of the turn, the Transponder antenna came into alignment with the water surface briefly and a few data points were collected at about 1.3 km distance. This data set is shown in Figure 8 with the GPS ground truth shown in red and the raw, unfiltered RF range measurements shown in blue. The range measurements are plotted on top of the GPS measurements, which are computed as a difference in position between the mobile GPS receiver and the surveyed location of the Originator antenna.

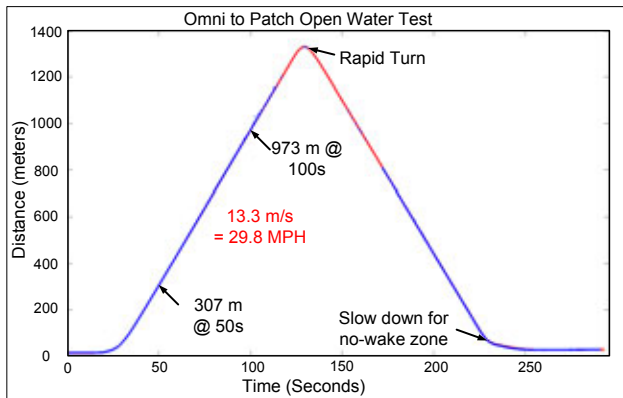


**Figure 8. Ski Boat Measurement Data**

This data shows high correlation between the GPS ground truth and the reported RF distance measurement.

To observe the performance of the ranging radios in an indoor environment, the radios were operated in the hallway of a surveyed office building using omnidirectional antennas within line-of-sight of each other. The Transponder was hand-held with the operator pausing at surveyed waypoints along the hallway. The measurement results from this test are shown in Figure 9 with raw, unfiltered RF range data in the blue traces and ground truth indicated during the stationary periods with red lines.

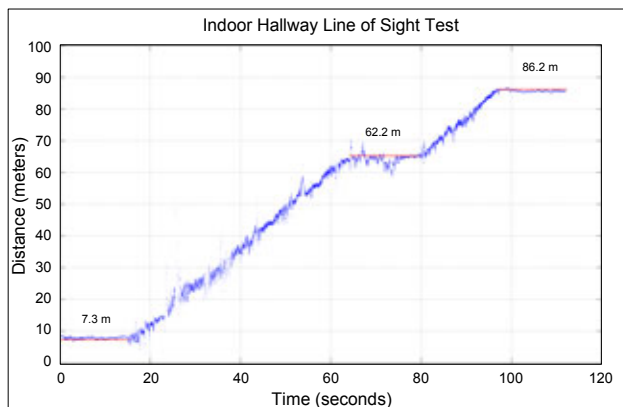


**Figure 9. Indoor Test Results**

In summary, these test results demonstrate that these RF distance measuring radios perform extremely well in benign RF, line-of-sight environments with reduced performance in more challenging environments. An ongoing topic of research for this project is to improve the performance of the distance estimation in all environments.

## CRAMER-RAO LOWER BOUND

The fundamental limitation on ranging performance in the presence of additive white Gaussian noise (AWGN) is described by the Cramer-Rao Lower Bound (CRLB). Although this is not the limiting factor in high-multipath environments, it provides a useful tool for benchmarking performance and estimating theoretical performance limitations. In this section, we present a detailed treatment of the CRLB for this system, which corrects a previously reported equation in [4].

In a simple edge-detection system, the CRLB can be expressed [3, 4] as Equation 1, where  $BW$  is the spectral bandwidth occupied by the signal in Hertz and  $E_s/N_o$  is the signal energy to noise density ratio.

$$\sigma_i^2 \geq \frac{1}{(2\pi \cdot BW)^2 \frac{E_s}{N_o}} \left( 1 + \frac{1}{\frac{E_s}{N_o}} \right) \quad (1)$$

The signal to noise density ratio  $E_s/N_o$  is related to the SNR as Equation 2, where  $t_s$  is the duration during which the signal occupies the spectral bandwidth  $BW$ .

$$SNR = \frac{P_s}{P_n} = \frac{E_s}{N_o} \frac{1}{t_s \cdot BW} \quad (2)$$

In other words,  $t_s$  is the length of time during which the signal was observed while it was doing something “meaningful,” such as changing in value. Systems with a  $(t_s \times BW)$  product greater than unity are considered to have “processing gain.” These systems are often implemented using pseudorandom number sequences that have some duration  $t_s$  over which several transitions occur and are observed. If a single PN sequence is observed, then  $t_s$  is simply the length in time of the PN sequence. If multiple PN sequences are observed, then  $t_s$  is extended further. This processing gain is not unlimited, as platform dynamics, clock stability, and other issues place a practical upper limit for the maximum  $t_s$  in any real system. We can write  $t_s$  as Equation 3 with  $a$  copies of the PN sequence consisting of  $N$  chips occurring at a chipping rate of  $f_{Chip}$ .

$$t_s = \frac{N \cdot \alpha}{f_{Chip}} \quad (3)$$

The CRLB for the variance of a one-way time-of-flight measuring system with processing gain can be therefore expressed as Equation 4.

$$\sigma_i^2 \geq \frac{1}{(2\pi \cdot BW)^2 \left( SNR \cdot N \cdot \alpha \cdot \frac{BW}{f_{Chip}} \right)} \quad (4)$$

In this RF ranging system, the time-of-arrival baseband phase computation is performed twice, once on the receive side of each radio to augment a coarse round-trip estimation based on clock cycle dwell times in both radios. In total, four measurements are performed:

- The dwell time in the Originator,  $M_{Count,Originator}$ ,
- The dwell time in the Transponder,  $M_{Count,Transponder}$ ,
- The baseband phase on receive side in the Transponder at the synchronization word,  $E_{Peak,Transponder}$ , and
- The baseband phase on the receive side in the Originator,  $E_{Peak,Originator}$ .

A “coarse time” estimate is obtained by normalizing the dwell times by the local baseband clock frequencies and computing their difference along with a calibrated offset  $t_{Delay}$ , as shown in Equation 5.

$$t_{Coarse} = \frac{M_{Count,Originator}}{f_{Originator}} - \frac{M_{Count,Transponder}}{f_{Transponder}} - t_{Delay} \quad (5)$$

For this system, the coarse counts may be computed exactly and the local clock frequencies are known to sufficient precision that this estimate can be assumed to be only limited by the precision or accuracy of the calibrated offset. A coarse distance measurement that is therefore not limited in practice by the CRLB, but is limited to the resolution of a baseband clock cycle can be computed as Equation 6.

$$d_{Coarse} = t_{Coarse} \frac{c}{2} \quad (6)$$

A fine correction factor can be computed from the baseband phase measurements normalized by their local clock frequencies as shown in Equation 7.

$$\begin{aligned} t_{FineAdjust} &= \frac{E_{Peak,Originator}}{f_{Originator}} + \frac{E_{Peak,Transponder}}{f_{Transponder}} \\ &= t_{Adjust,Originator} + t_{Adjust,Transponder} \end{aligned} \quad (7)$$

These two independent measurements are combined to form the final round trip time-of-flight computation, as shown in Equation 8.

$$\begin{aligned} d_{Round-Trip} &= \left( t_{Coarse} - t_{FineAdjust} \right) \frac{c}{2} \\ &= \left( \frac{t_{Coarse}}{2} - \frac{t_{Adjust,Originator} + t_{Adjust,Transponder}}{2} \right) c \end{aligned} \quad (8)$$

Each baseband phase correction factor estimate  $t_{FineAdjust}$  is constrained by the one-way CRLB of Equation 4. The CRLB of this system can be determined as the averaging of two independent one-way time-of-flight estimates. If the  $t_{Coarse}/2$  term is known exactly to clock-cycle precision, the CRLB for the variance of the distance measurement arises solely from the phase estimates, and is halved compared to Equation 4, as shown in Equation 9,

$$\sigma_d^2 \geq \frac{c^2}{2 \cdot (2\pi \cdot BW)^2 \left( SNR \cdot N \cdot \alpha \cdot \frac{BW}{f_{Chip}} \right)} \quad (9)$$

There is no additional factor of 4 improvement to the CRLB for variance arising from a round-trip measurement (due to a  $(c/2)^2$  term) as this measurement is considered two independent one-way measurements to correct each calculated dwell time. With  $BW = 2 \times f_{Chip}$ , the performance limit of the standard deviation for a distance estimate in this system can be expressed as Equation 10.

$$\sigma_d \geq \frac{c}{4\pi \cdot BW \sqrt{SNR \cdot N \cdot \alpha}} \quad (10)$$

The CRLB for the standard deviation of distance measurement for this RF ranging system can be estimated with  $BW = 22$  MHz,  $SNR = 10$  dB,  $\alpha = 42$  symbols observed, and  $N = 13$  chips, yielding 1.5 cm. This bound is well within a factor of two of our best measured outdoor performance, which suggests that this ranging method approaches the performance of a maximum likelihood estimator.

## CONCLUSION

A FCC-compatible high-precision software-defined ranging radio operating in the 2.4 GHz ISM band has been presented. The ranging method is primarily a function of baseband implementation and therefore this system migration from our previous work at 915 MHz to 2.4 GHz was straightforward. The digital radio system has been improved from a development kit-based

brassboard implementation to a custom radio suitable for further research and development. The implemented method retains its simplistic model of channel effects but achieves robust performance in low-multipath environments. Research is under way to improve the ranging system robustness and accuracy.

## ACKNOWLEDGMENTS

The authors would like to recognize Derek Pyner, Russ Fretenburg, and Henry Leung at Pacific Design Engineering, Inc. for development work supporting this project.

## REFERENCES

- [1] B. D. Farnsworth and D. W. A. Taylor, "High precision narrow band RF ranging," *Institute of Navigation International Technical Meeting (ION ITM '10)*, San Diego, California, 2010.
- [2] B. D. Farnsworth and D. W. A. Taylor, "Precision Software Defined DSSS Radio Frequency Ranging," *IEEE Sensors Conference 2010*, Waikoloa, Hawaii, 2010.
- [3] S. D. Lanzisera, "RF Ranging for Location Awareness," Doctoral dissertation, University of California, Berkeley, 2009.
- [4] S. D. Lanzisera, D. Lin, and K. Pister, "RF Time of Flight Ranging for Wireless Sensor Network Localization," *Workshop on Intelligent Solutions in Embedded Systems (WISE '06)*, Vienna, Austria, 2006.
- [5] D. W. A. Taylor, W. Todd Faulkner, and B. D. Farnsworth, "Precision RF Ranging as an Aid to Integrated Navigation Systems," *Institute of Navigation Global Navigation Satellite Systems (GNSS '10)*, Portland, Oregon, 2010.
- [6] D. W. A. Taylor and P. N. Johnson, "Innovative approach to local area precise positioning using direct sequence spread spectrum," Institute of Navigation National Technical Meeting, Anaheim, California, January 2003.
- [7] D. J. Pyner, R. A. Fretenburg, S. J. Kazemir, "Systems and methods for determining the distance between two locations," U.S. Patent No. 6,067,039, May 2000.
- [8] "OSSIE: SCA-Based Open Source Software Defined Radio," Available: <http://ossie.wireless.vt.edu/> [Accessed January, 2011].